Nonlinear resonant ultrasound spectroscopy (NRUS) applied to damage assessment in bone

Marie Muller[a)]
Laboratoire d'Imagerie Paramétrique, CNRS, Université Paris 6, 15 Rue de l'Ecole de Médecine, 75006 Paris, France

Alexander Sutin[b)]
Davidson Laboratory, Stevens Institute of Technology, Hoboken, New Jersey 07030

Robert Guyer[c)]
Department of Physics, University of Massachussets, Amherst, Massachussets 4525

Maryline Talmant[d)] and Pascal Laugier[e)]
Laboratoire d'Imagerie Paramétrique, CNRS, Université Paris 6, 15 Rue de l'Ecole de Médecine, 75006 Paris, France

Paul A. Johnson[f)]
Geophysics, MS D443, Los Alamos National Laboratory of the University of California, Los Alamos, New Mexico 87545

(Received 25 May 2005; revised 23 September 2005; accepted 24 September 2005)

Nonlinear resonant ultrasound spectroscopy (NRUS) is a resonance-based technique exploiting the significant nonlinear behavior of damaged materials. In NRUS, the resonant frequency(ies) of an object is studied as a function of the excitation level. As the excitation level increases, the elastic nonlinearity is manifest by a shift in the resonance frequency. This study shows the feasibility of this technique for application to damage assessment in bone. Two samples of bovine cortical bone were subjected to progressive damage induced by application of mechanical cycling. Before cycling commenced, and at each step in the cycling process, NRUS was applied for damage assessment. For independent assessment of damage, high-energy x-ray computed tomography imaging was performed but was only useful in identifying the prominent cracks. As the integral quantity of damage increased, NRUS revealed a corresponding increase in the nonlinear response. The measured change in nonlinear response is much more sensitive than the change in linear modulus. The results suggest that NRUS could be a potential tool for micro-damage assessment in bone. Further work must be carried out for a better understanding of the physical nature of damaged bone and for the ultimate goal of the challenging *in vivo* implementation of the technique. © *2005 Acoustical Society of America.* [DOI: 10.1121/1.2126917]

PACS number(s): 43.80.Qf, 43.80.Ev, 43.25.Ba, 43.25.Gf [FD] Pages: 3946–3952

I. INTRODUCTION

The diagnosis of bone fragility is currently obtained through the measurement of bone mineral density (BMD) obtained from x-ray densitometric techniques.[1] BMD is well known as a good predictor of bone strength[2] and is considered to be the best clinical technique for fracture risk prediction.[1] Other structural or material bone characteristics have been recognized as independent predictors of bone strength. Microdamage in bone is such a factor and strength degradation due to damage accumulation is of major clinical importance. Several studies have revealed a strong correlation between micro-damage and bone fragility, suggesting the importance of micro-damage assessment.[3,4] However, *in vivo* micro-damage has remained relatively poorly documented due to the lack of noninvasive techniques for its assessment.

Micro-damage is induced *in vivo* in bone by daily cyclic loading. This fatigue damage is considered to be one of the factors controlling the local stimulus for bone turnover, and the resulting remodeling results in repair of the resulting fatigue damage.[3] When an imbalance takes place in the remodeling process, micro-damage accumulates as micro-cracks,[3,5] with typical dimension of 5 to 400 μm. Osteoporotic bones are more micro-damaged than healthy bones.[6] It has been shown that fracture risk and correspondingly micro-crack density increases exponentially with age, with a higher rate for women than for men.[7–9] Fatigue damage has consequences on bone mechanical properties. It has been demonstrated that micro-damage accumulation coincides with a decrease of bone toughness[4] or stiffness.[10] Moreover, some data suggest a negative exponential relationship between bone strength and micro-crack density.[5] These results suggest

[a)]Electronic mail: muller@lip.bhdc.jussieu.fr
[b)]Electronic mail: asutin@stevens-tech.edu
[c)]Electronic mail: guyer@physics.umass.edu
[d)]Electronic mail: talmant@lip.bhdc.jussieu.fr
[e)]Electronic mail: laugier@lip.bhdc.jussieu.fr
[f)]Electronic mail: paj@lanl.gov

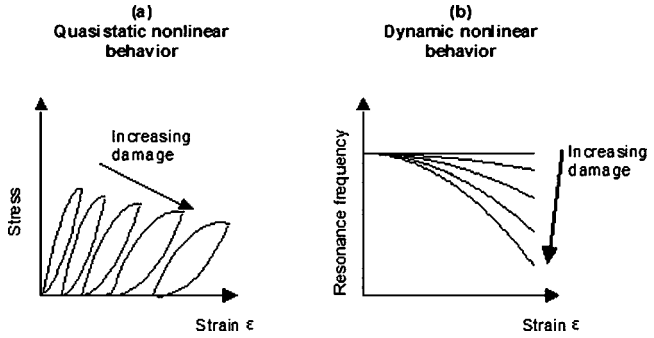

FIG. 1. (a) Stress-strain behavior of bone as a function of damage under quasitstatic conditions. (b) Resonance peak shift as function of strain amplitude, with increasing damage.

that micro-damage accumulation and bone fragility are related. *In vivo* micro-damage assessment could therefore provide important information regarding skeletal status and fracture risk. To date, two techniques are used for the assessment of fatigue damage in bone: histological measures of damage accumulation using staining techniques[11,12] and optical techniques such as micro-computed tomography. However, both are limited to the measurement of *in vitro* specimens. Indeed, dimensions of micro-cracks in bone (5 to 400 μm)[13,14] are such that the resolution needed for the imaging devices to detect them requires very high energy levels, difficult and dangerous to apply *in vivo*. It is therefore crucial to develop a damage assessment technique that could be used *in vivo*.

Accumulation of damage in bone leads to a stress-strain behavior that is correspondingly more nonlinear than in healthy bone.[15,16] In other words, as fatigue damage accumulates in bone, the stress-strain curve exhibits an increasingly pronounced bend and an increased hysteresis[17] [Fig. 1(a)], which may be a manifestation of a softening of the bone, due to a larger crack density. As damage level increases the corresponding nonlinear dynamical behavior manifests itself as a larger decrease in the resonance frequency for a given wave amplitude [Fig. 1(b)]. The decrease in resonance frequency corresponds to a decrease in modulus and wave speed. We hypothesize that the nonlinearity in the stress-strain relation may be exploited in the assessment of damage in bone as it has been elsewhere. Indeed, it is now well known that damaged materials, as well as consolidated and unconsolidated inhomogeneous materials, display a characteristic, elastic-nonlinear behavior, termed simultaneously "nonlinear mesoscopic," "nonclassical nonlinear," "nonequilibrium," and "anomalous" behavior.[18–20] From empirical evidence it is clear that micro-cracks in materials are responsible for the enhanced nonlinear response, acting as an ensemble of soft inclusions in a rigid matrix. This is referred to as the "hard/soft" paradigm of nonclassical nonlinear materials.[18,21,22] This is the reason why nonlinear elastic wave techniques are in development for nondestructive evaluation (NDE) and damage assessment in a very large group of materials. Nonlinear resonant ultrasound spectroscopy (NRUS) is one of those techniques and has proved to be valuable for damage detection because of its high sensitivity.[18,20,23,24] It is important to note that, while nonlinear methods are extremely sensitive to the presence of damage, we have no quantitative link between damage quantity and nonlinear response, although significant effort is being directed to this issue. Currently, empirical relations can be derived for specific materials providing the means to infer damage quantity from nonlinear response. The objective of this study was to explore for the first time the potential of nonlinear resonant ultrasound spectroscopy to assess progressively induced bone damage.

II. THEORY

Recent, careful studies carried out on rock under well-controlled conditions (constant temperature and in an atmosphere of nitrogen gas)[25] showed that, at low strains, "nonclassical" materials behave classically, exhibiting Duffing oscillator behavior (a perturbation expansion of the stress-strain describing nonlinear dynamics[26]). Above strains of roughly 10^{-6}, it is currently thought that macro- and micro-cracks, as soft mesoscopic structural features in a rigid matrix, are responsible for a characteristic nonlinear response related to the presence of strain memory and hysteresis in the stress-strain relation, the equation of state (EOS). Although the underlying physical mechanisms are not well understood, Guyer and McCall proposed a phenomenological description of these nonlinear effects,[21,27] considering the material as an ensemble of individual elastic units, some hysteretic and some not. In damaged bone, micro-cracks could play the role of these hysteretic units. The individual hysteretic units are recorded in the Preisach-Mayergoyz space (PM space), which provides the means to track the behavior of the ensemble of hysteretic units for a given stress history applied to the material. A one-dimensional EOS can be derived from the density of hysteretic units in PM space,[27]

$$\sigma = \int K(\varepsilon, \dot{\varepsilon}) d\varepsilon, \tag{1}$$

where σ is stress, ε is strain, $\dot{\varepsilon}$ is the strain rate, and K is the elastic modulus of the material,

$$K = K_0(1 + \beta\varepsilon + \delta\varepsilon^2) - \alpha(\varepsilon, \dot{\varepsilon}), \tag{2}$$

where K_0 is the linear modulus, ε is the strain and α is the hysteretic nonlinear parameter that depends on the strain derivative $\dot{\varepsilon}$ due to the hysteresis. The corresponding wave equation expresses the driving force for the local displacement as a function of the strain,

$$\ddot{u} = \frac{K_0}{\rho}\frac{\partial}{\partial x}(\Delta\varepsilon + \beta\Delta\varepsilon^2 + \delta\Delta\varepsilon^3 + \cdots) + \alpha(\Delta\varepsilon, \dot{\varepsilon}), \tag{3}$$

where $\ddot{u}$ is the particle acceleration, ρ is the material density, and $\Delta\varepsilon$ is the average strain over a wave cycle. The nonlinear parameters β and δ describe the classical nonlinear terms due to standard anharmonicity, although the material damage contributes to these terms in nonlinear mesoscopic materials. The hysteretic nonlinear parameter in the model, α, dominates the nonlinear behavior at large drive strains as noted above and it is relatively straightforward to track its behavior as the sample is progressively damaged and becomes more elastically nonlinear.[20,28] This phenomenon can be understood as a softening of the material when the excitation level

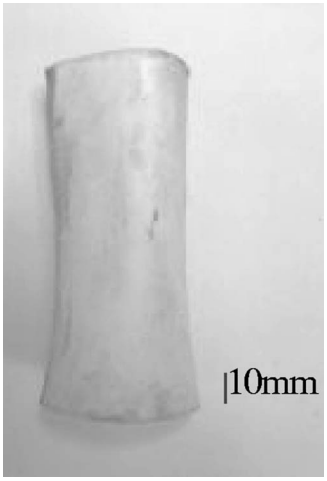

FIG. 2. Bone sample B1. The end surfaces are flat and parallel.

increases, which becomes more pronounced with accumulated damage. It can be shown from Eq. (3) that

$$\frac{\Delta f}{f_0} = \frac{f - f_0}{f_0} \approx \alpha \Delta \varepsilon, \tag{4}$$

where f is the linear resonance frequency and f_0 is the resonance frequency at the lowest (linear) drive level[23] for a given resonance mode. Thus from the frequency shift as a function of strain, we can extract α. As noted, there is no quantitative relationship between α and damage as yet; however, much empirical evidence shows a clear link.[18–23] The model is functional for our purposes here, but we note that, in its original formulation, it does not account for "slow dynamics," the recovery process that occurs in these materials after large amplitude wave excitation, nor for the process of "conditioning," strain-memory that takes place during application of NRUS.[21]

III. EXPERIMENTAL PROCEDURE

A. Samples

The study was carried out on two bovine femur specimens. After removing soft tissue and marrow, the samples were soaked in a 2% saline solution with a dish degreaser and wrapped in gauze in order to keep them hydrated during the experiment. The samples were machined frozen in a lathe in order to obtain flat and parallel surfaces at the sample ends for transducer placement. The two samples (termed B1 and B2) had a tubular shape, with an approximate wall thickness of 8 and 11 mm, respectively, and an approximate diameter of 49 and 46 mm, respectively. Both samples were 116 mm long. They were cut in the central part of the diaphyseal shaft and were approximately symmetrical compared to the midshaft line (see Fig. 2).

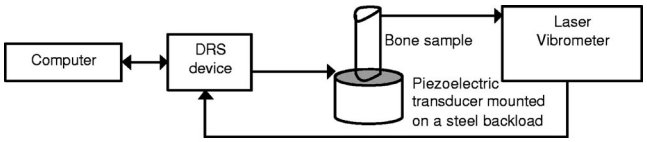

FIG. 4. Experimental setup for the NRUS experiment.

B. Fatigue

A progressive damage experiment was carried out in 11 steps (termed here steps 0 to 10, step 0 corresponding to the intact sample). The samples were progressively damaged by compressional fatigue cycling in an INSTRON 5569 press. For the first eight cycling sessions, the samples were cycled 60 times, to a maximum stress of 15 Mpa at a rate of 30 Mpa/min (about 1 h cycling). For the last two sessions, they were cycled 80 times to a maximum stress of 25 Mpa at a rate of 40 Mpa/min (about 1 h 40 min cycling, see Fig. 3).

C. Nonlinear resonant ultrasound spectroscopy (NRUS)

At each damage step, NRUS experiments were performed on the samples, using a resonant ultrasound spectroscopy device (Dynamic Resonance Systems, Inc., Powell, WY, USA). Each sample was probed using a step-sweep in frequency around a resonance mode of the sample. The modal peak frequency was determined, and the process was repeated at gradually increasing drive levels. The experimental setup used for the NRUS is shown in Fig. 4. To obtain large wave amplitudes, a resonator was constructed using a large piezoelectric transducer (77-mm diameter, 6-mm thickness) mounted with epoxy to a thick, 5180 steel backload (77-mm diameter, 51-mm thickness). The source was coupled to the specimens by application of phenyl salicylate. The source produced the desired large amplitudes; however, because of the coupled resonators (backload and bone sample), the measured resonance spectrum was complex. Therefore modeling was carried out in order to determine which resonance modes would provide information related to the bone sample rather than the backload, and thus be relevant for the NRUS experiment. The analytical model was

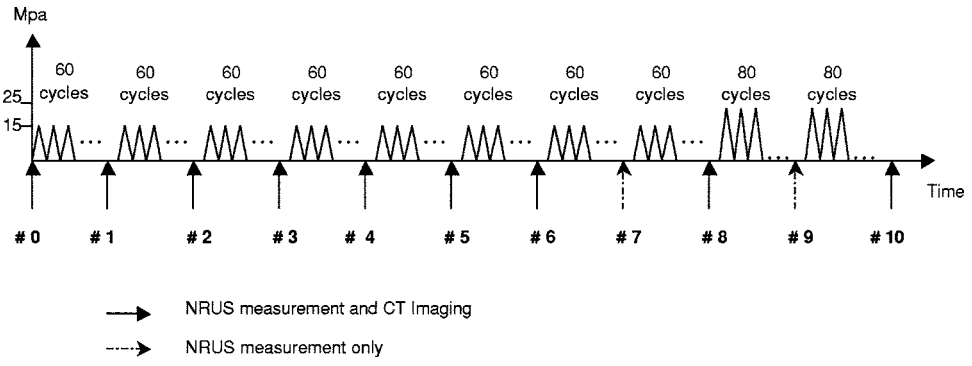

FIG. 3. Stress protocol for the progressive damage experiment.

for unidimensional propagation in two adjacent media (backload and bone), separated by a thin transducer generating forced oscillations at the interface between the two medias, mimicking the actual setup. Displacement at the bottom of the backload was fixed to zero (the backload was considered to be sitting on a rigid substrate) and the extremity of the bone was considered free. The simulation showed that the 42-kHz peak corresponded to a resonance mode of the bone sample and was well separated from adjacent modes. This resonance mode was selected for further study because the separation allows one to analyze the resonance frequency peak shift without overlap of adjacent peaks (which can influence the location and width of the peak).

Particle velocities related to the longitudinal displacement at the top, and the radial displacement on the side of the bone sample were measured using a laser vibrometer (Polytec OFV 3001 with the OFV 303 Sensor Head). Small pieces of aluminum foil were glued to the samples tops and sides in order to increase the reflectivity of the laser vibrometer and thereby increase the signal-to-noise ratio. Longitudinal dynamic strain amplitude ε_L is calculated from the measured particle velocity, $\varepsilon_L = \partial u/\partial x = \dot{u}/2\pi f L$, where f is the frequency and L is the length of the sample (116 mm). Radial strain is related by Poisson's ratio, meaning it is approximately $\varepsilon_L/4$.

Linear resonance has a long history of development and application for measurement of wave velocity and attenuation. For instance, Bolef and colleagues developed standing wave resonance techniques applying nonlinear (electronic) mixing to determine the wave velocity in materials.[29,30] Starting in the 1980s, the resonant ultrasound spectroscopy (RUS) technique was introduced to measure the full elastic tensor of solids.[31] The NRUS technique presented here is the extension of those two experimental methods to nonlinear elasticity, where the resonance (spectral) peak is used to extract the material nonlinear parameter and could potentially be used to extract the nonlinear parameter tensor.

D. Computed tomography (CT) imaging

High-energy x-ray, three-dimensional computed tomography (CT) was performed (x-ray cabinet model FCT-2252 with a 225 kV micro-focus source, Hytec Inc, Los Alamos, NM, USA), in order to have an independent assessment of damage in the samples. CT images were reconstructed with a pixel size of 127 μm. This resolution only allowed us to detect the larger cracks. CT imaging experiments were carried out for steps 0, 1, 2, 3, 4, 5, 6, 8, and 10.

IV. RESULTS

For each damage step, the resonance curves around 42 kHz were measured for increasing amplitudes of the drive level. Figure 5 shows an example of resonance curves, obtained by measuring the radial velocity close to the top of sample B1, and corresponding CT images, for damage steps 0 and 9.

As drive level increased, a shift in the resonance frequency could be observed at all damage steps. The resonant peak shift was, however, more significant in the progressively damaged stages [Fig. 5(b)] than in the undamaged sample [Fig. 5(a)]. α was then extracted according to Eq. (3).

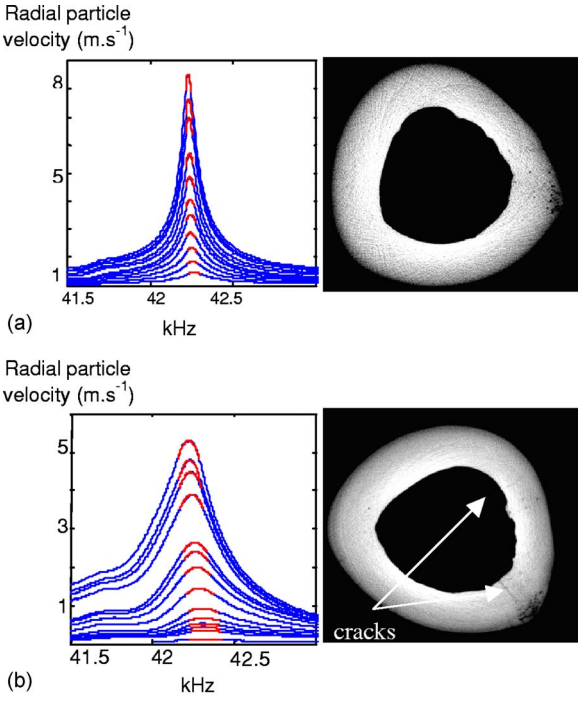

FIG. 5. (Color online) Example of resonance curves for damage steps 0 and 9. The radial velocity measured close to the top of sample B1 is plotted as a function of frequency. Top: damage step 0, Bottom: damage step 9.

Figure 6 illustrates the behavior of the frequency shift as a function of average strain for samples B1 [Fig. 6(a)] and B2 [Fig. 6(b)]. Each curve corresponds to a damage step. Some of the steps were eliminated due to poor experimental conditions (poor coupling primarily). The slope of the curves is very close to one for all steps and both samples, as the theory predicts (sample B1: mean=0.99, standard deviation =0.02, range=0.95–1; sample B2: mean=1.01, standard deviation=0.02, range=0.99–1.03).

As the amount of damage increases in the samples, the curves shift upward in the frequency-strain space, indicating an increased nonlinear signature meaning there is more frequency shift for the same strain interval.

Figure 7 shows the behavior of the speed of sound in the samples (derived from the linear resonance frequency f_0 at each step) and the nonlinear parameter α as a function of damage step for the two samples. As damage accumulates, the speed of sound c ($c=f_0\lambda$ where f_0 is the linear resonance frequency and λ is the wavelength) is almost constant (although a slight decrease can be observed in sample B2 when damage increases). On the other hand, α dramatically increases with the accumulated damage but its behavior is not the same for the two samples. In B1, the increase of α is almost linear ($\alpha \approx 1.17\#\text{step} + 0.86$) whereas the behavior in B2 is fit by a higher-order polynomial function ($\alpha \approx 0.05\#\text{step}^3 - 0.56\#\text{step}^2 + 2.13\#\text{step} - 0.96$). The different dependencies indicate that cumulative damage was not the same for the same quantity of cycling. The difference between linear and nonlinear measurements is remarkable.

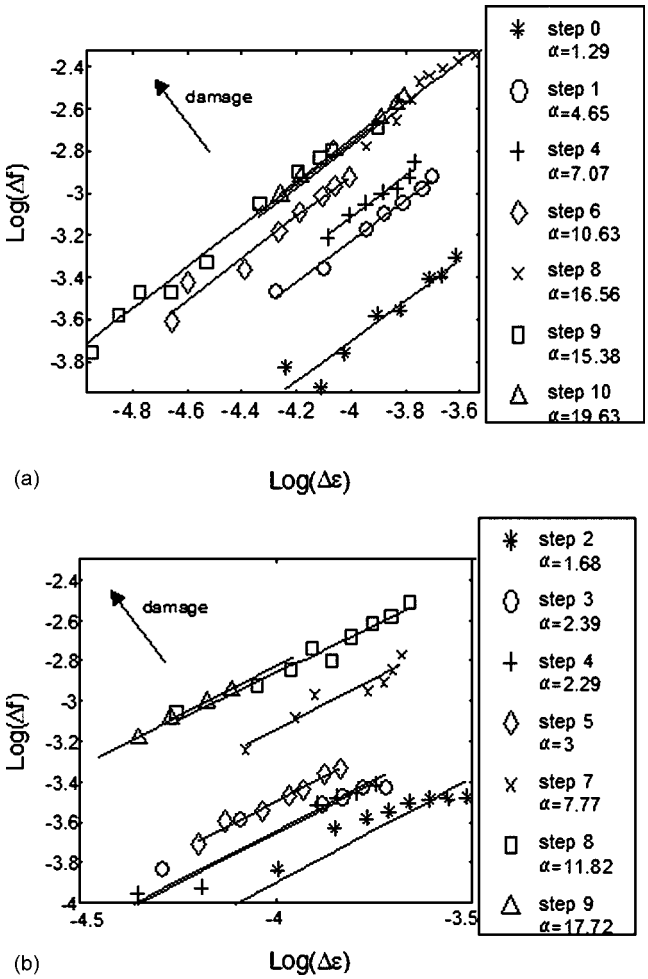

FIG. 6. Resonance frequency shift as a function of strain in log-log space. As damage increases, the curves are translated towards the top of the space, reflecting an increasing nonlinear parameter.

V. DISCUSSION

The primary purpose of this work was to demonstrate for the first time the feasibility of nonlinear resonant ultrasound spectroscopy techniques to detect progressive damage in bone. This was accomplished in a progressive damage experiment, in which the NRUS technique provided the means to characterize damage in bone via the nonlinear hysteretic parameter α.

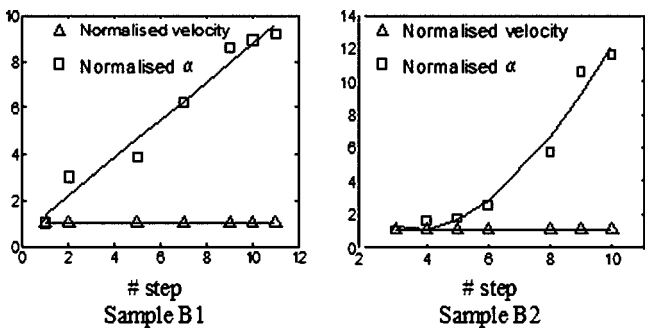

FIG. 7. Nonlinear parameter α (squares) and velocity (triangles) normalized to the nonlinear parameter and velocity for the "intact" sample, as a function of damage step in the two samples (left: sample B1, right: sample B2).

A. Resonance curves, hysteretic behavior

Figure 5 indicates that a small resonance frequency shift occurs in the "intact" sample. This result was expected, considering the fact that intact, healthy bone contains continually healing micro-cracks and remodeling as noted in the Introduction. Moreover, intact bone by itself could be classified as a nonlinear mesoscopic elastic material, because of its heterogeneous mesoscopic structure. As noted above, the α parameter measured in this study reflects damage accumulation, or relative damage, rather than an absolute quantity of damage. This has been demonstrated in numerous other materials as well.[23]

B. Imaging

In order to have an independent assessment of the damage mechanically induced in the samples, CT imaging was performed at different damage steps. Images of the same slice of sample B1 are shown in Fig. 5. Some cracks are visible in Fig. 5(b) (damage step 9 in sample B1) that are not present in the intact sample [Fig. 5(a), damage step #0 in sample B1]. The resolution of the images (the pixel size is 127 μm) does not allow for a quantification of microdamage since micro-cracks lengths in bone are in a range of 5 to 400 μm. Higher resolution imaging methods are required for comparative quantification.

C. Wave dissipation

Figure 5 shows a change in the wave dissipation, reflected by the fact that the curves obtained during progressive damage cycling are broader than the curves obtained from the "intact" state. A measure of the wave dissipation, given by the Q of the material, has been shown to be very useful for assessing nonclassical behavior, and thus the relative quantity of damage in a material.[22] Unfortunately, we were unable to exploit the Q observations because of inconsistent results. We suspect that the aluminium foil (glued on the sample to increase reflectivity for the laser vibrometer) was not always bonded properly to the sample, and that additional vibration of the foil could have influenced the width of some of the resonance curves (although not the frequency). It is also possible inconsistencies in the source bonding at each step influenced the Q.

D. Anisotropy

Changing the orientation of the laser vibrometer provided the means to measure two different velocities: the longitudinal particle velocity, measured on the top of the sample, and the radial particle velocity, measured on the side of the sample. The results presented in this paper only employed the radial velocity. Indeed, no consistent result could be found with the longitudinal particle velocity. Damage formed under compressive loads applied along the longitudinal bone axis has consistently been associated with the appearance of oblique shear cracks.[32] One possible interpretation to our results is that the effect of damage on mechanical properties is anisotropic and that the particle velocity in one direction (e.g., longitudinal) is less sensitive than in the other

direction (e.g., radial). An intensive modeling effort must be conducted, along with additional experiments, to understand this phenomenon.

E. Nonlinear hysteretic parameter

Figure 6 shows the behavior of the frequency shift as a function of the maximum amplitude strain for each damage step. The slopes of all the curves are about 1, for the two samples. This result is predicted by the theory. Indeed, Eq. (3) implies a linear relation between Δf and $\Delta\varepsilon$. As damage is induced in the samples, the curves move upward in $\Delta f/f_0$-strain-space, indicating an increasing nonlinear hysteretic parameter.

The behavior of α and the speed of sound as a function of damage is illustrated in Fig. 7. The result is impressive: clearly, the nonlinear parameter α measured by NRUS is much more sensitive to damage than the speed of sound, related to the Young's modulus of the material which stays nearly constant during the entire progressive damage experiment (only a very slight decrease is observable for sample B2). α begins to increase at the first damage step, even though damage is not yet discernable on the x-ray CT images. To date, quantitative ultrasound (QUS) techniques give access to parameters such as speed of sound (SOS) and attenuation in bone. These parameters being mainly related to bone mineral density (BMD) have already proved their efficacy in the assessment of fracture risk.[33,34] A recent experimental study reported the failure of SOS and attenuation to reflect mechanically induced damages in cancellous bone.[35] This observation is also supported by our results, showing that NRUS actually allows for micro-damage detection in bone with a sensitivity much higher than that of SOS.

For sample B1, the relation between α and the number of damage steps is almost linear whereas a third-order polynomial fits the data from sample B2. This may be related to the fact that damage did not occur in the same manner in the two samples, even though they were both cycled following an identical protocol. The two samples may not have been in the same damage state at step 0, or perhaps we are seeing an indication of the natural variability of how bone responds to induced damage. An independent quantitative evaluation of micro-damage (higher resolution imaging like micro-CT for example) would have been useful here to determine a semi-quantitative relation between the measured nonlinear parameter α and micro-damage. This will be done in future work. The other limitation of this study is the small number of data points. Indeed, the number of damage steps is not sufficient to correctly understand the shape of the curves shown in Fig. 7. In any case, the trend is clearly demonstrated in this work: there is a strong relation between micro-damage and the nonlinear hysteretic parameter α. We are currently conducting a study using a large number of human bone samples, with a larger number of damage steps.

A number of challenging difficulties have to be considered before the technique can be applied noninvasively, *in vivo*. Among them are bone excitation by means of an external mechanical vibration and recording the vibration by means of a remote sensor. Vibro-acoustic spectrography using the acoustic radiation force as an external source and a hydrophone as a remote sensor might be a tempting solution.[36] Other important factors to be considered will be the relation of bone to other organs (joint, tendons) and the influence of soft tissue surrounding bone that are likely to significantly change the resonance characteristics.

VI. CONCLUSIONS

This is the first study showing the feasibility of nonlinear resonant ultrasound spectroscopy to detect damage in bone. A progressive damage experiment has been conducted on two samples of bovine bone. The increasing amount of damage mechanically induced in the sample leads to an increased shift in the resonance frequency with wave amplitude, indicating a progressively more nonlinear behavior of the sample as the sample damage accumulates. This study allowed for the determination of a parameter relevant for bone damage assessment: the nonlinear hysteretic parameter, related to the resonance frequency shift. This work is a preliminary study and some aspects, such as the fact that only the radial displacement is sensitive to damage, are not well understood yet. For an accurate quantification of damage in human bone, the experiments must be repeated, with a larger number of data points. This work is in progress and will allow for the assessment of a quantitative relationship between bone micro-damage and the nonlinear hysteretic parameter. Further work will have to be carried on for the *in vivo* application of the technique to see if it may be viable as a diagnostic tool for skeletal status assessment.

ACKNOWLEDGMENTS

This work was supported by Institutional Support (LDRD) and by the Institute of Geophysics and Planetary Physics at Los Alamos, and the Centre National pour la Recherche Scientifique (CNRS, France). The authors would like to acknowledge J. Tencate, T. Darling, and P. Zysset for helpful discussions and comments.

[1]Consensus development conference: diagnosis, prophylaxis, and treatment of osteoporosis," Am. J. Med. **94**, 646–650 (1993).
[2]J. C. Rice, S. C. Cowin, and J. A. Bowman, "On the dependence of the elasticity and strength of cancellous bone on apparent density," J. Biomech. **21**, 155–168 (1988).
[3]R. Martin, "Fatigue Microdamage as an Essential Element of Bone Mechanics and Biology," Calcif. Tissue Int. **73**, 101–107 (2003).
[4]P. Zioupos, "Accumulation of in-vivo fatigue microdamage and its relation to biomechanical properties in ageing human cortical bone," J. Microsc. **201**, 270–278 (2001).
[5]D. B. Burr, M. R. Forwood, D. P. Fyhrie, R. B. Martin, M. B. Schaffler, and C. H. Turner, "Bone microdamage and skeletal fragility in osteoporotic and stress fractures," J. Bone Miner. Res. **12**, 6–15 (1997).
[6]A. M. Parfitt, "Bone age, mineral density, and fatigue damage," Calcif. Tissue Int. **53**(Suppl. 1), S82-5; discussion S85-6 (1993).
[7]M. B. Schaffler, K. Choi, and C. Milgrom, "Aging and matrix microdamage accumulation in human compact bone," Bone (N.Y.) **17**, 521–525 (1995).
[8]T. L. Norman and Z. Wang, "Microdamage of human cortical bone: incidence and morphology in long bones," Bone (N.Y.) **20**, 375–379 (1997).
[9]B. Martin, "Aging and strength of bone as a structural material," Calcif. Tissue Int. **53**(Suppl. 1), S34-9; discussion S39-40 (1993).
[10]M. B. Schaffler, E. L. Radin, and D. B. Burr, "Mechanical and morphological effects of strain rate on fatigue of compact bone," Bone (N.Y.) **10**, 207–214 (1989).

[11]D. B. Burr and T. Stafford, "Validity of the bulk-staining technique to separate artifactual from in vivo bone microdamage," Clin. Orthop. Relat. Res. **260**, 305–308 (1990).
[12]F. J. O'Brien, D. Taylor, and T. C. Lee, "An improved labelling technique for monitoring microcrack growth in compact bone," J. Biomech. **35**, 523–526 (2002).
[13]D. Taylor, "Microcrack growth parameters for compact bone deduced from stiffness variations," J. Biomech. **31**, 587–592 (1998).
[14]F. J. O'Brien, D. Taylor, and T. C. Lee, "Microcrack accumulation at different intervals during fatigue testing of compact bone," J. Biomech. **36**, 973–980 (2003).
[15]D. B. Burr and C. H. Turner", "Biomechanics of bone," Ame. Soc. Bone Min. Res., 58–64 (2003).
[16]D. Jepsen, Akkus, "Observation of Damage in Bone," in *Bone Mechanics Handbook* (CRC Press, 2001).
[17]D. R. Carter, W. E. Caler, D. M. Spengler, and V. H. Frankel, "Fatigue behavior of adult cortical bone: the influence of mean strain and strain range," Acta Orthop. Scand. **52**, 481–490 (1981).
[18]R. A. Guyer and P. A. Johnson, "Nonlinear Mesoscopic Elasticity: Evidence for a new class of materials," Phys. Today **52**, 30–35 (1999).
[19]L. Ostrovsky and P. Johnson, "Dynamic nonlinear elasticity in geomaterials," Riv. Nuovo Cimento **24**, (2001).
[20]K. V. D. Abeele, A. Sutin, J. Carmeliet, and P. A. Johnson, "Micro Damage diagnostics using nonlinear elastic wave spectroscopy (NEWS)," NDT & E Int. **34**, 239–248 (2001).
[21]R. A. Guyer and K. R. McCall, "Hysteresis, Discrete Memory, and Nonlinear Wave Propagation in Rock: A New Paradigm," Phys. Rev. Lett. **74**, 3491–3494 (1995).
[22]P. A. Johnson and A. Sutin, "Slow dynamics and anomalous nonlinear fast dynamics in diverse solids," J. Acoust. Soc. Am. **116**, 124–130 (2004).
[23]K. V. D. Abeele, J. Carmeliet, J. A. Tencate, and P. A. Johnson, "Nonlinear Elastic Wave Spectroscopy (NEWS) Techniques to Discern Material Damage, Part II: Single-Mode Nonlinear Resonance Acoustic Spectroscopy," Res. Nondestruct. Eval. **12**, 31–42 (2000).
[24]P. A. Johnson, B. Zinszner, P. Rasolofosaon, F. Cohen-Tenoudji, and K. V. D. Abeele, "Dynamic measurements of the nonlinear elastic parameter in rock under varying conditions," J. Geophys. Res. **109**, B02202 (2004).
[25]J. A. Tencate, D. Pasqualini, S. Habib, K. Heitmann, D. Higdon, and P. A. Johnson, "Nonlinear and nonequilibrium dynamics in geomaterials," Phys. Rev. Lett. **93**(6), 065501 (2004).
[26]J. J.Stoker, *Nonlinear Vibrations in Mechanical and Electrical Systems* (Intersciences, New York, 1950).
[27]K. R. McCall and R. A. Guyer, "Equation of state and wave propagation in hysteretic nonlinear elastic materials," J. Geophys. Res. **99**, 23887–23897 (1994).
[28]R. A. Guyer, K. R. McCall, and K. V. D. Abeele, "Slow elastic dynamics in a resonant bar of rock," Geophys. Res. Lett. **25**, 1585–1588 (1998).
[29]D. I. Bolef and J. G. Miller, "High Frequency Continuous Wave Ultrasonics," Phys. Acoust., 95–201 (1971).
[30]J. G. Miller and D. I. Bolef, "A 'sampled-continuous wave' ultrasonic technique and spectrometer," Rev. Sci. Instrum. **40**, 915–920 (1969).
[31]R. G. Leisure and F. A. Willis, "Resonant ultrasound spectroscopy," J. Phys.: Condens. Matter **9**, 6001–6029 (1997).
[32]W. T. Dempster and R. T. Liddicoat, "Compact bone as a non-isotropic material," Am. J. Anat. **91**, 331–362 (1952).
[33]D. Hans, L. Genton, S. Allaoua, C. Pichard, and D. O. Slosman, "Hip fracture discrimination study: QUS of the radius and the calcaneum," J. Clin. Densitom. **6**, 163–172 (2003).
[34]M. L. Frost, G. M. Blake, and I. Fogelman, "A comparison of fracture discrimination using calcaneal quantitative ultrasound and dual X-ray absorptiometry in women with a history of fracture at sites other than the spine and hip," Calcif. Tissue Int. **71**, 207–211 (2002).
[35]P. H. Nicholson and M. L. Bouxsein, "Quantitative ultrasound does not reflect mechanically induced damage in human cancellous bone," J. Bone Miner. Res. **15**, 2467–2472 (2000).
[36]M. Fatemi and J. F. Greenleaf, "Ultrasound-stimulated vibro-acoustic spectrography," Science **280**, 82–85 (1998).